# Diffraction Effects

W. G. Bagnuolo, Jr.
CHARA, Georgia State University, Atlanta, GA 30303

## E.1. INTRODUCTION

Diffraction effects may be significant over long distances, even for a wide beam. Therefore, unless care is taken, diffraction effects can seriously degrade the performance of an interferometric array. Previously, Tnago and Twiss (1980) considered diffraction effects for a small diameter interferometer. Visibility losses were tabulated as a function of the pathlengths of the two combining beams *e.g.* from 200 and 400 m respectively.) The flatness of the wavefronts assumed made it possible to calculate the wavefront analytically with only one numerical quadrature. More recently, Hrynevych (1992) has extended these results with more mathematical rigor and experimental verification, and has considered the specific case of the SUSI (Sydney University Stellar Interferometer). For beams with aberrations due to atmospheric turbulence, analytic solutions seem very difficult, and none have been published to date. Therefore, numerical calculations from scalar diffraction theory (including various formulations) have been used to estimate visibility losses. An earlier version of this work (Bagnuolo 1988) "diffracted" model atmospheres numerically to examine the losses in visibility in an interferometer as a function of beam size.

For the CHARA there are two wavebands of interest: 0.55–0.9 $\mu$m ($\approx$V, R, and I) and 2.1–2.4 ($\approx$K). Therefore, we need to consider diffraction effects for three cases:

- K-band observations, in which we are in the single-$r_0$ regime without AO,
- Visual bands observations with an (AO) system,
- Visual bands without AO, limited to "1-2 $\times$ $r_0$" apertures (*i.e.* 20–30 cm).

Ideally, one would like to reduce the beam size as much as possible in order to reduce the size and cost of the optics, especially the Optical Path Length Equalizer (OPLE). There is therefore a trade-off between the beam reduction factor and the losses in visibility (and other effects) due to diffraction. In the CHARA array the beam reduction factor of 8:1 thus represents a compromise.

In the rest of this Appendix we will briefly summarize scalar diffraction theory, the simulations, and the implications for the CHARA Array.

## E.2. SCALAR DIFFRACTION THEORY RESULTS

Because of the long pathlengths the Fresnel approximation is valid and thus (Goodman 1968):

$$U(x_0, y_0) = \frac{e^{jkz}}{j\lambda z} \int U(x_1, y_1) e^{\left\{\frac{jk}{2z}[(x_0-x_1)^2+(y_0-y_1)^2]\right\}} dx_1, dy_1$$

or

$$U(x_0, y_0) = \frac{e^{jkz}}{j\lambda z} U(x_1, y_1) * e^{\frac{jk(x^2+y^2)}{2z}} \tag{E.1}$$

where $U(x_0, y_0)$ is the (scalar) amplitude at the output plane and $U(x_1, y_1)$ is the amplitude at the input plane, $z$ is the distance, and * represents convolution.

The second relation expresses the output amplitude as the convolution of the input with an oscillatory phase function. The problem with this formulation computationally is that for moderately large $x$ and $y$ the oscillatory function varies significantly over a pixel and is difficult to estimate (and to compute the convolution via a fast Fourier transform.)

An equivalent formulation is in terms of angular frequency (with a different notation from Goodman):

$$u(f_x, f_y, 0) = F[U(x_1, y_1, 0)]$$

$$u(f_x, f_y, z) = u(f_x, f_y, 0) H(f_x, f_y)$$

$$U(x_0, y_0, z) = F^{-1}[u(f_x, f_y, z)] \tag{E.2}$$

where we start with the input plane at $z$=*0*, and take its Fourier transform to get the angular spectrum, $u(f_x, f_y, o)$. The angular spectrum at a propagation distance $z$ can be found by multiplying the initial angular spectrum by a function:

$$H(f_x, f_y) = e^{\left[\frac{j2\pi z}{\lambda}\sqrt{1-(\lambda f_x)^2-(\lambda f_y)^2}\right]} \;=\; 0, \quad \text{if} \;\; f_x^2 + f_y^2 > 1/\lambda^2. \tag{E.3}$$

Finally, the angular frequency at $z$ is reversed transformed to get the (complex) amplitude.

If we look at the expression for $H$, we note that the maximum spatial frequency in, say, $f_x$ is $\leq 1/\lambda$ or for $\lambda = 550$ nm, the maximum $f_x = 1.8 \times 10^6 \mathrm{m}^{-1}$. For a reasonable pixel size and wavefront irregularities of interest $f_x \approx 50 - 100\ \mathrm{m}^{-1} \ll f_x(max)$ so that the following approximation in Equation E.3 can be made. For small $b$, $\sqrt{1-b} \approx 1 - 1/2b$, so

$$H(f_x, f_y) \approx e^{(j2\pi z/\lambda)} e^{[-j\pi z\lambda(f_x^2+f_y^2)]} \tag{E.4}$$

The first argument is just the (absolute) phase along the beam and is irrelevant. For $\lambda = 550$ nm and $f_x = 100$ the argument in the second exponential reaches $\pi$ at about 200 m. The slower variation of the argument in Equation E.4 is a computational advantage of this formulation compared to Equation E.1. As Hrynevych (1992) points out, this general formulation of scalar diffraction theory has the advantage of being able to directly use the fast Fourier transform (FFT).

A number of diffraction calculations were made using equations Equation E.3 and E.4 and the FFT as a preliminary check. A square aperture with a simulated aperture of 1 meter (1 cm/pixel 128 x 128 pixel grid) was propagated from 100- 3200 m. The results were compared to the well-known results via the *Cornu spiral* (Jenkins & White 1957). In all cases the intensities produced by Equation E.3 and Equation E.4 agreed with the exact results to within 1%.

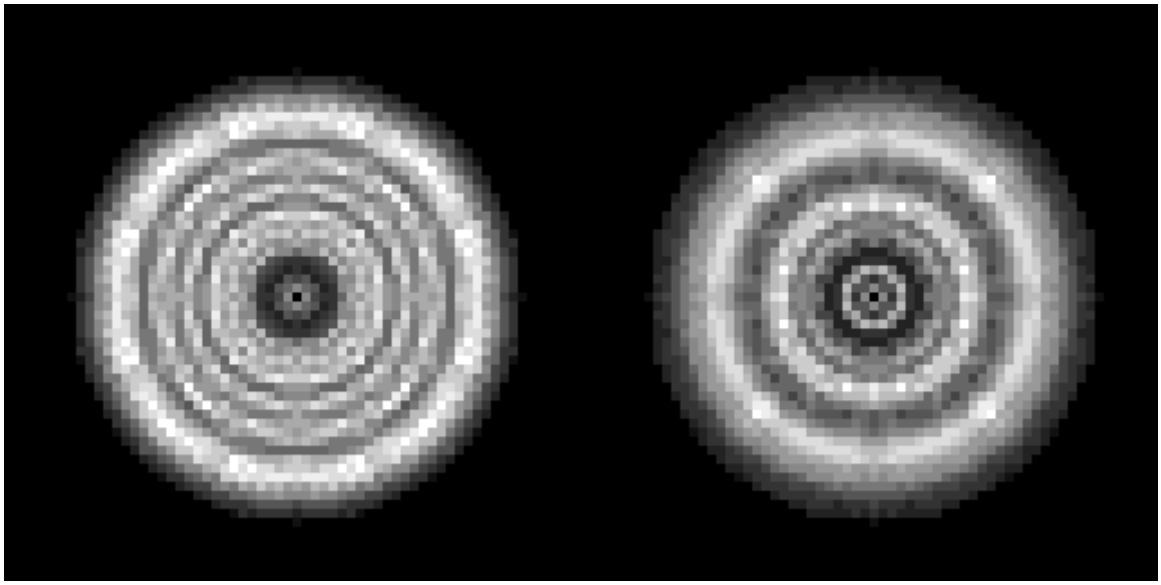

**FIGURE E.1.** Intensities for beams at 2.2 $\mu$m of 1 m diameter reduced to 125 mm and propagated for 100 m (left) and 200 m (right).

## E.3. SOME EXAMPLES OF DIFFRACTION EFFECTS

In the proposed long baseline interferometer, beams will be not just transmitted via siderostats, but reduced in diameter. Compared to the simple circular case, an added effect is the diffraction produced by the central hole in the primary, which creates a series of smaller waves like the primary's edge. Another more important effect is due to the magnification. A heuristic way of looking at the situation is that, first, diffracted rays are created at the edges of the primary aperture. The angles of all rays, including the diffracted rays, are then magnified by a factor of $m$. For the current CHARA design $m = 8$. Thus the effect of magnification is to increase the spread of diffraction waves absolutely by a factor of $m$. But, because the size of the beam is reduced by $1/m$, the net effect of magnification is to increase the diffraction effects relative to the beam by a factor of $m^2$. Thus, diffraction may become a serious problem if $m$ is too large. (Note that by the same type of argument as above, diffraction effects vary only linearly with the distance).

We consider first diffraction effects on a flat wave ($r_0$ very large).

Figure E.1 shows the diffraction pattern from an flat wavefront at 2.2 $\mu$m into a 1.0 m aperture telescope, reduced to a 12.5 cm beam and propagated for 100 and 200 meters respectively. Figure E.2 shows the corresponding intensity cross-sections of these beams.

The "ringing" in these beams can be quelled by apodization, for the price of a loss of light. The cross-section of the beam can be modified by a kind of Hamming window, *i.e.*, the transmission may be written:

$$t(n) = 0.54 - 0.46\cos(\pi(50 - n)/\Delta n), \qquad 50 - \Delta n \le n \le 50 \qquad \text{(E.5)}$$

where *t(n)* is the transmission at pixel $n$ from center (Note the nominal radius of $n =$ 50 cm), and $\Delta n$ is the transition bandwidth. This sort of window makes a smooth taper

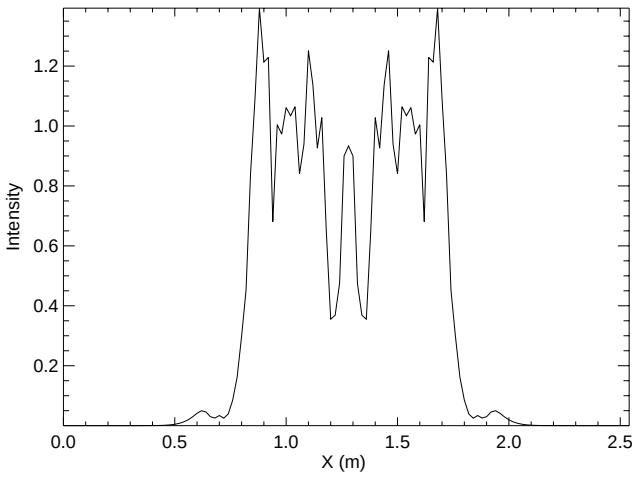


**FIGURE E.2.** Intensity cross-section for beam at 2.2 $\mu$m of 1 m diameter reduced to 125 mm and propagated for 100 m.

between 0.08 transmission at the edge and 100% transmission at $n = 50 - \Delta n$. Figure E.3 shows the result of an apodized beam with $\Delta n$ =8 cm propagated as in Figure E.1. Note the improvement, at a cost of about 16% in lost light.

## E.4. DIFFRACTION EFFECTS ON THE CHARA ARRAY

The three relevant cases to the CHARA Array are:

- K-band observations, in which we are in the single-$r_0$ regime without AO.
- Visual band observations with an (AO) system,
- V-band without AO, limited to "1-2 $\times$ $r_0$" apertures (*i.e.* 20-30 cm.

In order to evaluate diffraction effects on the CHARA Array, first an atmospheric phase-plate model (Bagnuolo 1988) is constructed out of a finite number of waves (51 in this model) whose spatial frequencies $k_n$ are distributed at uniform logarithmic intervals, and $1/L_0 < k_n < 1/l_0$, where ($L_0 \approx 100$ m and $l_0 \approx 1$ mm). The amplitudes are deterministic and chosen to give the Kolmogorov structure function. Wave directions ($\theta_n$) and phase shifts ($\phi_n$) are randomly chosen.

Wavefronts are next "propagated" through two telescopes and light-combining optics for given pathlengths. Model wavefront can be corrected for tilts and other abberations. The two beams are combined in terms of complex amplitude via a "beamsplitter", in which the reflected beam is retarded by $\pi$ radians. Another set of output beams is created by creating a $\pi/2$ delay in the second beam before combining. Tango & Twiss (1980). Then an estimate of the visibility is given by

$$I_{jkr} = I_0[1 + (-1)^j \gamma \cos(\phi_k + r\pi/4)] \tag{E.6}$$

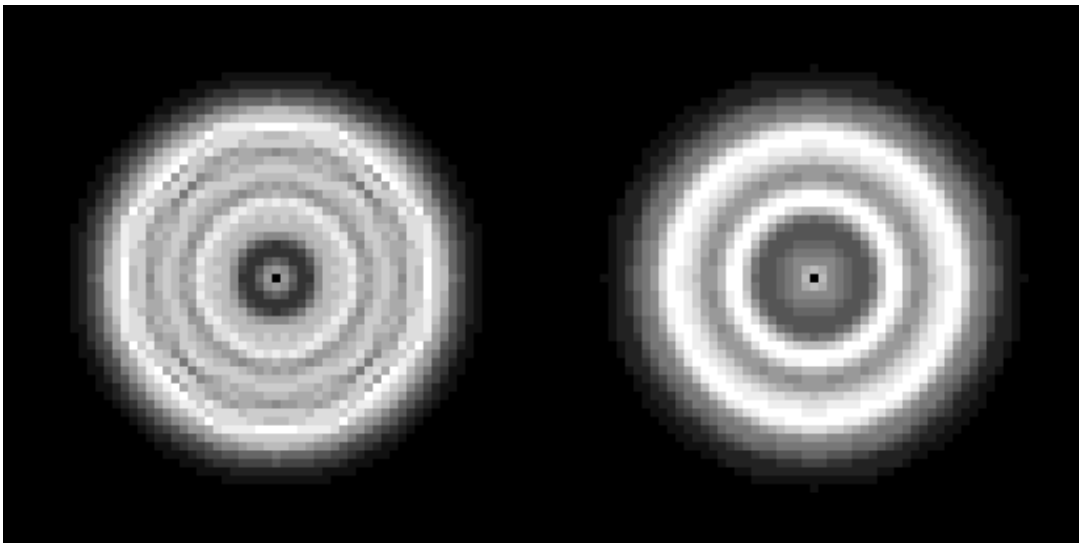

**FIGURE E.3.** Intensities for beams at 2.2 $\mu$m of 1 m diameter reduced to 125 mm and propagated for 100 m (left) and 200 m (right). Beams are apodized with $\Delta$n = 8 cm.

where

j=1,2 are the two pupil planes

r=0,1 (with/without the $\pi/4$ phase switch

k= 1 to m, observation no.

$I_0$ is the mean intensity.

Let:

$$q = 1/m \sum_{k=1} n(N_{1k0} - N_{2k0})^2 + (N_{1k1} - N_{2k1})^2 \qquad \text{(E.7)}$$

### E.4.1. The K-band IR Case

Figure E.5 shows the result of one simulated visibility measurement for the IR case, in which the propagation distances were $d_1 = 100$ and $d_2 = 200$ m respectively. The seeing was $r_0(V)$= 20 cm, or $r_0(K)$=106 cm (very good).

Table E.1 shows visibilities and diffraction-induced losses for several cases in the IR. In these simulations the average of twenty sets of phaseplates were used. The visibility is estimated from $V \approx (V^2)^{1/2}$. Some comments on these results: First, the typical worst case for the IR normally is the (100,200)m case from configuration B, but we can operate in configuration A in the IR with small visibility losses. [It was shown in Tango (1980) and Hyrenevich (1992) that the worst visibility losses from diffraction occur from somewhat unequal configurations, such as (100,200) m rather than equal lengths like (200,200) m.] Secondly, to maintain high visibility without AO it is necessary to stop down the aperture somewhat during mediocre seeing. Thirdly, with full aperture under mediocre seeing (and reduced visibility) diffraction losses are somewhat less. Finally, in the worst cases at least 10% of the light is diffracted beyond the original edge of the aperture [the fifth column lists normalized intensities of the combined beams inside the original aperture relative to the no-diffraction case).

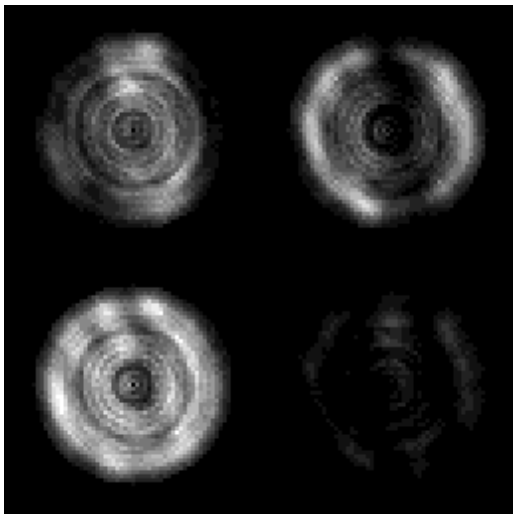

**FIGURE E.4.** Intensities for four output beams at 2.2 $\mu$m under very good seeing propagated for 100 m (left) and 200 m (right).

### E.4.2. The Visual Band Case with No AO

In the visual bands with no AO, sub-apertures must be used in order to obtain an adequately high visibility under normal conditions.

Figure E.5 shows the result of one simulated visibility measurement for the visual case (at 700 nm) in which the propagation distances were $d_1 = 100$ and $d_2 = 200$ m respectively. The seeing was $r_0(0.55\mu m)$= 20 cm.

Table E.2 shows visibilities and diffraction-induced losses for several cases in the visual bands. In the visual-band cases, diffraction losses are relatively small under favorable seeing conditions. Under mediocre conditions, with long pathlengths visibility losses can approach 0.10. This is probably still acceptable, as long as it is taken into account via calibrations. There is a bit of improvement for diffraction losses if a larger aperture (at lower visibility) is used.

### E.4.3. The Visual Band Case with AO

In the visual bands with an AO system, the whole 100 cm aperture can be used. If the compensation is perfect (flat wavefront), there is little loss of visibility for diffraction at visual wavelengths for the CHARA array.

Figure E.6 shows the result of one simulated visibility measurement for a flat wavefront at 550 nm in which the propagation distances were $d_1 = 200$ and $d_2 = 400$ m respectively.

Table E.3 shows visibilities and diffraction-induced losses for several cases in the visual bands with an AO system. In order to simulate imperfect AO systems, a residual fractional wavefront error, denoted by $\epsilon$ has been left in the models. (*i.e.* $\epsilon$ =0.10 means that 90% of the wavefront error has been successfully corrected by the AO system.

**TABLE E.1.** Visibilities for IR Cases.

| $r_0$(K) (cm) | Aperture ) (cm) | $d_1$ (m) | $d_2$ (m) | I (norm) | V | $\Delta$V |
|---|---|---|---|---|---|---|
| 106 | 100 | 0 | 0 | 1.000 | 0.867 | 0.000 |
| | | 100 | 200 | 0.917 | 0.848 | 0.019 |
| | | 200 | 400 | 0.879 | 0.841 | 0.026 |
| 53 | 100 | 0 | 0 | 1.000 | 0.642 | 0.000 |
| | | 100 | 200 | 0.918 | 0.643 | -0.001 |
| | | 200 | 100 | 0.872 | 0.647 | -0.004 |
| 53 | 75 | 0 | 0 | 1.000 | 0.740 | 0.000 |
| | | 100 | 200 | 0.999 | 0.713 | 0.027 |
| | | 200 | 400 | 1.028 | 0.686 | 0.054 |

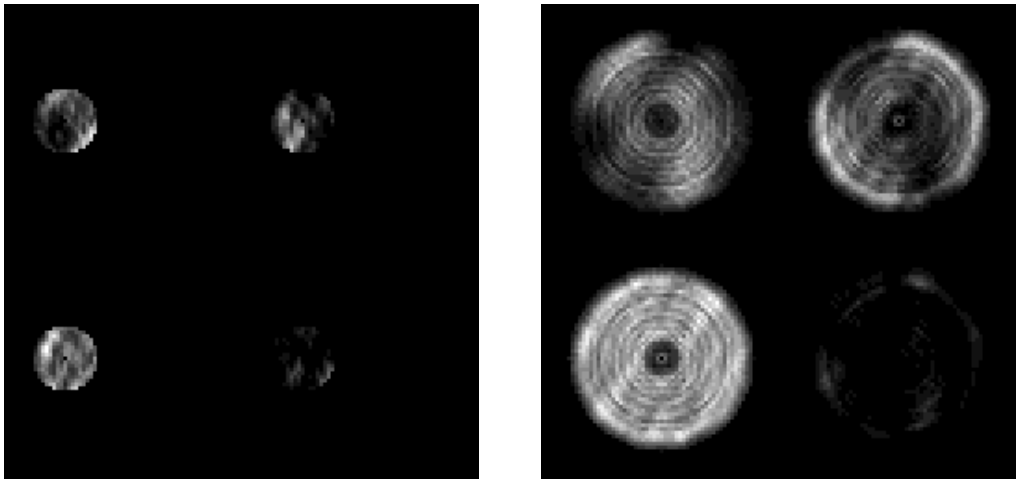

**FIGURE E.5.** (Right) Intensities for four output beams at 700 nm under very good seeing with 35 cm apertures propagated for 200 and 400 m. (Left) Intensities for four outbeams with AO System with residual error $\epsilon$=0.25

**TABLE E.2.** Visibilities for Visual Band Cases, no AO.

| $r_0(V)$ (cm) | $\lambda$ (cm) | Aperture ) ($\mu$m) | $d_1$ (m) | $d_2$ (m) | I (cm) | V (norm) | $\Delta$V |
|---|---|---|---|---|---|---|---|
| 20 | 0.55 | 20 | 0 | 0 | 1.000 | 0.862 | 0.000 |
| | | | 200 | 400 | 1.010 | 0.802 | 0.060 |
| 20 | 0.55 | 30 | 0 | 0 | 1.000 | 0.757 | 0.000 |
| | | | 200 | 400 | 1.014 | 0.715 | 0.042 |
| | | | 300 | 600 | 1.002 | 0.702 | 0.055 |
| 10 | 0.55 | 15 | 0 | 0 | 1.000 | 0.743 | 0.000 |
| | | | 200 | 400 | 0.979 | 0.632 | 0.111 |
| 10 | 0.70 | 20 | 0 | 0 | 1.000 | 0.753 | 0.000 |
| | | | 200 | 400 | 0.996 | 0.656 | 0.097 |
| 10 | 0.70 | 25 | 0 | 0 | 1.000 | 0.694 | 0.000 |
| | | | 200 | 400 | 1.001 | 0.599 | 0.095 |

**TABLE E.3.** Visibilities for Visual Band Cases, with AO.

| $r_0(V)$ (cm) | $\lambda$ ($\mu$m) | $\epsilon$ | $d_1$ (m) | $d_2$ (m) | I (cm) | V (norm) | $\Delta$V |
|---|---|---|---|---|---|---|---|
| 10 | 0.70 | 0.25 | 0 | 0 | 1.000 | 0.785 | 0.000 |
| | | | 200 | 400 | 0.942 | 0.777 | 0.008 |
| 20 | 0.70 | 0.30 | 0 | 0 | 1.000 | 0.885 | 0.000 |
| | | | 200 | 400 | 0.943 | 0.871 | 0.014 |

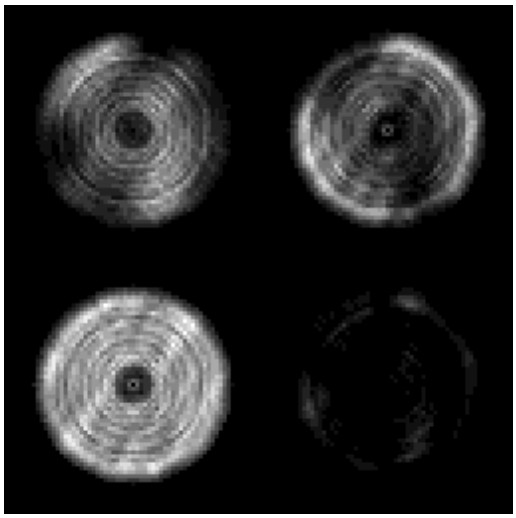

**FIGURE E.6.** Intensities for four output beams at 0.55 $\mu$m under AO system with 25% residual error.

## E.5. CONCLUSIONS

The amount of diffraction effects in the system is proportional to the beam reduction factor squared and the propagation distance. There is therefore a tradeoff between the reduced cost of a smaller beam (in OPLEs, buildings, etc.) and losses in measured visibility due to diffraction effects. The latter are relatively small for the IR cases of interest, and insignificant for the visible-band AO cases. The worst cases are for the v-band (at 550 nm) without AO under mediocre seeing, and even then losses are acceptable and could be calibrated out.

## E.6. REFERENCES

Bagnuolo, W.G., "Simulations for the CHARA/GSU Interferometer and Binary Star Speckle Photometry" in NOAO-ESO *Conference on High Resolution Imaging by Interferometry,* Edited by B.R. Frieden, (Munchen: Springer-Verlag), 981

Goodman, J.W. 1968, *Introduction to Fourier Optics*, (New York: McGraw–Hill).

Hrynevych, M., 1992, *Diffraction Effects in Michelson Stellar Interferometry,* (PhD Thesis, University of Sydney)

Jenkins, F.A. & White, H.E. 1957, *Fundamentals of Optics*, (New York: McGraw–Hill).

Roddier, F. & Lena, P. 1984, *J. Optics* **15**, 171.

Tango, W.J. & Twiss, R.Q. 1980, *Progress in Optics* **17**, 240.